Comparison of atomic quasi-Landau spectrum with semiclassical strong-field-mixing models

Raymond J. Fonck,* F. L. Roesler, and D. H. Tracy
Physics Department, University of Wisconsin, Madison, Wisconsin 53706

Frank S. Tomkins
Chemistry Division, Argonne National Laboratory, Argonne, Illinois 60439

(Received 31 July 1979)

The authors compare the spectrum of the regularly spaced photoabsorption resonances which appear in the vicinity of the ionization threshold for atoms in a strong magnetic field with predictions of semiclassical strong-mixing models. Quasi-Landau resonance positions are shown to agree well with a two-dimensional WKB semiclassical hydrogenic model which depicts the resonances as bound states of the electron in the combined Coulomb and magnetic fields and which reduces to the Rydberg levels at low excitation. Simpler treatments based on a modified Bohr atomic model are also discussed. The data include observations in the $M = 0$ even-parity channels of Ba I and Sr I with $B = 25$–40 kG and the $M = -1$ odd-parity channel of Ba I at $B = 47$ kG. A scaling procedure is used to allow field-independent comparison among the various spectra and models. Although fairly successful in predicting energy positions, none of the models attempts to explain the complex resonance profiles or superposed fine structure, thus indicating the need for a comprehensive quantum-mechanical theory of the diamagnetic strong-mixing regime. The appearance of the quasi-Landau resonances in $M = 0$ even-parity spectra is consistent with the requirement that the states have even parity with respect to reflection along the direction of the magnetic field in order for the resonances to occur.

I. INTRODUCTION

Renewed interest in the behavior of free atoms in magnetic fields has arisen with the discovery of extremely high fields (up to 10^9 kG) in astrophysical objects such as neutron stars and with new laboratory observations of atomic spectra in strong external fields (~50 kG).[1-7] The diamagnetic term in the Hamiltonian for an atomic electron in the presence of an external magnetic field is the dominant magnetic interaction for loosely bound states. Three regimes of interest can be classified according to the relative values of the Coulomb interaction energy between an excited electron and the atomic core (E_c) and the magnetic interaction of the electron with an external magnetic field (E_m). At low excitation or weak magnetic fields, $|E_c| \gg |E_m|$ and the energy eigenvalues are the usual Coulomb levels with paramagnetic and diamagnetic perturbations. For free electrons in a uniform magnetic field (i.e., $|E_m| \gg |E_c|$), the usual Landau levels are obtained. The third and least understood regime is the strong-mixing regime, in which the Coulomb and diamagnetic interactions exert a comparable influence on the electronic motion (i.e., $|E_c| \approx |E_m|$).

The strong-diamagnetic-mixing regime covers the energy region in which the transition from Rydberg states to Landau levels occur as the level of excitation increases. Here perturbation theory is inadequate to calculate the eigenstates and eigenvalues of the system since the Coulomb and magnetic interactions are approximately equal in magnitude, and the theoretical analysis of this problem is quite complex and still in an early state of development. In practice, diamagnetic strong mixing can be observed in one-electron photoabsorption spectra near the ionization limit (or limits) for atoms in strong external magnetic fields. The dominant features of the spectrum in this energy region are series of approximately equally spaced resonances spanning the zero-field ionization limit. These resonances, originally discovered by Garton and Tomkins[8] in atomic barium, arise because the electron is trapped in a cylindrically symmetric harmonic potential for motion perpendicular to the magnetic field and far from the ionic core. They are conveniently referred to as quasi-Landau resonances (QLR).[9] Since the initial experiment of Garton and Tomkins, semiclassical models have been developed to describe the positions of quasi-Landau resonances as functions of energy and magnetic field strength.[2,3,9,10] The more complete of these models describe a continuous evolution of the energy eigenstates from the low-lying Coulomb levels, through the strong-mixing regime, to the Landau levels at very high excitation.

We have measured the positions of quasi-Landau resonances in the two-photon (even-parity) absorption spectra of strontium and barium, and our preliminary analysis demonstrated agreement between measurements and a two-dimensional Wentzel-Kramers-Brillouin (WKB) calculation of the

resonance positions.[7] In this paper, we examine further the correspondence between the WKB theory and our experimental results. In addition, we consider simpler semiclassical models that can be obtained from a modified Bohr atomic model. We find that all the models considered share a common scaling of parameters (such as energy E and principal quantum number n) with magnetic field strength, and this scaling allows a rather compact method of comparing experimental results with the various models. The acquisition of odd-parity absorption spectra of the barium principal series with $B = 47$ kG has extended our range of observations further above the ionization limit. We also note that the appearance of the quasi-Landau resonances in some polarizations but not in others is consistent with a selection rule derived from symmetry considerations.

II. EXPERIMENT

Most of the results discussed here were obtained via two-photon ionization spectroscopy.[11] A schematic diagram of our experimental apparatus is shown in Fig. 1. A nitrogen-laser-pumped dye laser is tuned to two-photon resonances from the ground state for the atomic species under study (in our case, either Ba I $^1S_0$ or Sr I $^1S_0$). After the transition to a highly excited state, the atom ionizes through a variety of processes including collisional, photo-, or chemi-ionization,[12] and the resulting ions are detected using a space-charge-amplified ionization detector. Recording this ion signal as the laser frequency is scanned yields the two-photon absorption spectrum.

A National Research Group Model 0.6-8-300 nitrogen laser was used. The dye laser consisted of a Hänsch-type oscillator with an intracavity Fabry-Perot etalon plus an amplifier dye cell. An external etalon between the oscillator and amplifier was also used, with a resulting linewidth of ~0.07 cm^{-1}. After collimation and polarization, the dye laser beam was focused into the center of an atomic vapor oven. The beam was linearly polarized with a Wollaston prism plus a compensating wedge, and a Babinet-Soleil compensator was used to rotate the plane of polarization without changing the laser intensity. The laser repetition rate was 30 pps, and peak power at oven center was estimated to have been $\gtrsim 10^6$ W/cm^2.

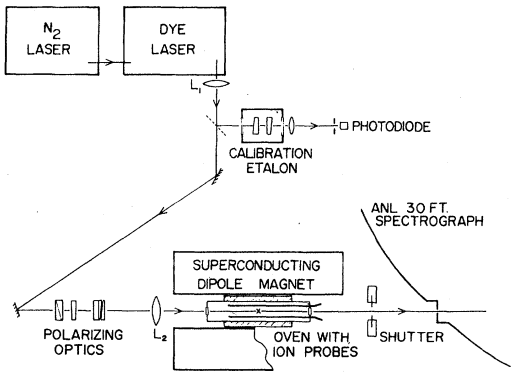

FIG. 1. Schematic diagram of the two-photon ionization spectroscopy experiment.

The dye laser frequency was varied by pressure scanning the oscillator and external etalon with SF_6 gas. Each scan covered a laser wave-number range of ~25 cm^{-1}. The relative laser wave number was monitored by recording the transmission of a sealed calibration etalon along with the ionization signal. Absolute laser wave number was determined to ± 0.02 cm^{-1} by intermittently opening an optical shutter which exposed a photographic plate on the Argonne National Laboratory 30-ft spectrograph. The resulting lines were compared to a thorium reference spectrum.

The atomic vapor oven was a resistively heated stainless steel tube with water-cooled ends. Oven windows were wedged to prevent the appearance of interference fringes in the signal. The buffer gas used was neon with $P_{Ne} \approx 10$ torr. The oven temperature was typically $T = 740$ °C for barium ($P_{Ba} \approx 0.1$ torr) and $T = 650$ °C for strontium ($P_{Sr} \approx 0.1$ torr). The oven was enclosed in a water-cooled copper jacket and the entire assembly was centered in the core of a superconducting dipole magnet which is capable of producing transverse fields up to $B = 40$ kG. The magnetic field strength as a function of magnet current was calibrated in an earlier experiment[13] using the Paschen-Back splittings of the $6snd\,^1D_2$ levels of Ba I.

The ion detector consisted of two parallel tungsten rods which extended the length of the oven and were positioned symmetrically about the oven axis in a plane parallel to the transverse magnetic field. These 1-mm diameter rods were separated by 1 cm. No auxiliary heating of the rods was required to obtain sufficient thermionic electron emission. A space-charge-limited current between the rods was established by biasing one rod slightly negative ($|V_{bias}| \leq 0.42$ V) with respect to the other, which was grounded to the oven wall. This current was passed through a load resister ($R = 60$ kΩ for the barium measurements, and $R = 310$ kΩ for strontium), and the resulting signal sampled by an ac-coupled boxcar integrator with an integration time per pulse of 2 msec and an output time constant of 0.3 sec, corresponding to an average over 9 laser pulses. This signal and the calibration etalon output were recorded on a strip-chart recorder.

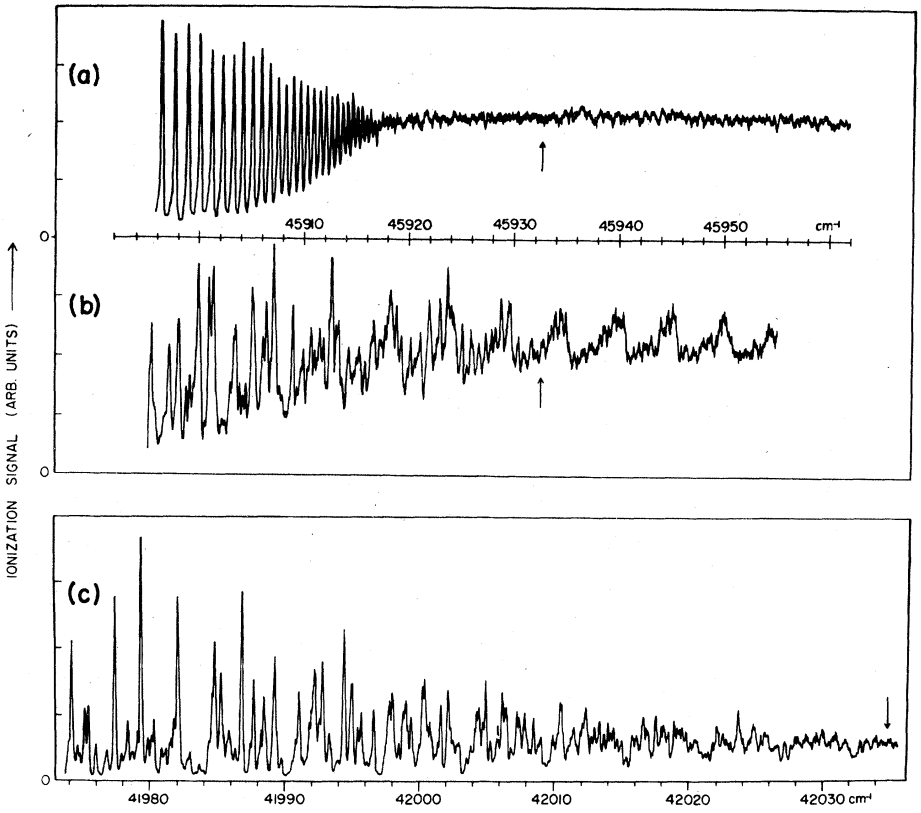

FIG. 2. Samples of two-photon (even-parity) ionization spectra in the region of the ionization limit (reproduced from Fig. 1 of Ref. 7). Zero-field ionization limits are marked by vertical arrows. (a) Sr I, $B=0$. The $5snd\,^1D_2$ series is seen converging to the Sr II $5s\,^2S_{1/2}$ limit at 45 932.19 cm^{-1}. (b) Sr I, $B=40.0\pm0.1$ kG, π polarization ($M=0$). (c) Ba I, $B=40.1\pm0.1$ kG, $M=0$. Intensity minima are visible below the Ba II $6s\,^2S_{1/2}$ limit at 42 034.85 cm^{-1} (Ref. 23).

Samples of two-photon spectra obtained near the first ionization threshold are shown in Fig. 2 for Ba I and Sr I. The noise level is due mainly to laser intensity fluctuations and is approximately the same percentage of the signal level for all three spectra in Fig. 2. When $B=0$, the spectrum near the ionization limit is dominated by the $ms^2\,^1S_0$-$msnd\,^1D_2$ ($m=5$ for Sr and $m=6$ for Ba) Rydberg series converging to the limit. When $B\neq0$, the quasi-Landau resonances appear as a low-frequency periodic intensity modulation in the spectrum spanning the entire region of the zero-field ionization limit.

Superposed on these diffuse resonances is complex, incompletely resolved sharp-line structure. This line structure, which is seen above the noise level extending up to and possibly across the limit, is quite sensitive to the value of B, but does reproduce provided that the magnetic field strength is accurately reproduced. The line structure is due to the diamagnetically raised and mixed even-parity nl Rydberg levels and is characteristic of the strong-diamagnetic-mixing regime for all polarizations.

The detailed structure of the QLRs will be influenced by motional Stark effects[14] due to electric fields induced by thermal molecular motion in the external magnetic field. This can affect individual line profiles, cause small line shifts[5] and, by breaking parity, introduce extra structure. Considerable structure in the Li I diamagnetic spectrum has been attributed[15] to motional Stark effects, but for the heavier species studied here the effects should be much less pronounced, particularly as regards the coarse features of the spectra.

In the present work, we concentrate on measurements of the positions of the quasi-Landau resonances and leave the much more complicated problem of the fine structure and resonance profiles to future investigations. For measurement purposes, we define the position of each resonance by its most identifiable feature. In barium, this is the intensity minimum, while for strontium we choose the peak of the sawtooth-shaped profile. Uncertainties in these measurements are due to noise and to the complicated fine structure superposed on the resonances, especially for the lower-energy region in strontium. The intensity minima in the barium spectra are fairly well defined, while resonance positions for the Sr I spectra were obtained by visually averaging over the fine structure present. Subjective estimates of the uncertainties of such measurements were typically

$\sim \pm 0.5$ cm^{-1}. The root-mean-square deviation of repeated measurements from their mean values was 0.2 cm^{-1} in the region of the ionization limit (-30 cm$^{-1} < E < 70$ cm^{-1}, where $E=0$ denotes the $B=0$ threshold) and we take this to be a reasonable estimate of the random error in a given measurement of a resonance position near $E=0$. Additional systematic uncertainties resulting from the variability of QLR profile shapes may be comparable or even greater. At $E \gtrsim 70$ cm^{-1}, the resonance positions are ill-defined due to low contrast, and information concerning their profiles is lost in the noise. At these higher energies, the uncertainty of a given resonance position measurement is estimated to be $\sim \pm 1$ cm^{-1}. The contrast of the resonances gradually decreases with increasing E until, for $B=40$ kG, their positions are not measurable for $E \gtrsim 100$ cm^{-1}.

For π polarization ($M=0$, where M is the total magnetic quantum number) and $B=40$ kG, the intensity modulations in the Ba I spectrum below the limit were identifiable down to the diamagnetic configuration mixing regime where the $6s31s\ ^1S_0$ level is still identifiable. At these lower energies, there is an energy interval in which the definition of the resonances is ambiguous as the spectrum evolves from the diamagnetically shifted nl Rydberg levels into the strongly mixed region with the quasi-Landau modulations. However, this interval has a width of only about one resonance spacing and so poses no serious problem for the present study.

Data obtained at various field strengths allowed the positions of individual resonances to be followed over the range $B=25$–40 kG. No resonances were observed above the noise level for $B \leq 20$ kG. No periodic intensity modulations were clearly observed in σ polarization, but any resonances present were probably obscured by the superposition of the $M=0$, $+2$, and -2 spectra.

In addition to the two-photon ionization data, photographic absorption spectra for the $6s^2\ ^1S_0$–$6snp\ ^1P_1{}^0 (M=-1)$ principal series of Ba I were obtained by one of the authors (FST) using a superconducting solenoid magnet.[16] In Fig. 3, we present a densitometer recording of a plate in the region above the first ionization limit for $B=47$ kG. A barium oven was operated as a heat pipe with $P_{Ba}=3$ torr; the background continuum was obtained from a heavy-current hydrogen tube. Over the last several years, many such plates have been obtained at Argonne for several different elements over a wide range of magnetic field strengths, and we include the single spectrum of Fig. 3 in our discussion in order to extend our range of observations to energies well beyond those obtained with the laser data.

In the spectrum of Fig. 3, the resonances near the limit are obscured by saturation of the absorption in the vapor. At reduced vapor pressure ($P_{Ba} \approx 0.7$ torr), however, these resonances have been traced back to the $B=0$ ionization limit. In the $E \approx 0$ region, fine structure is superposed on the quasi-Landau modulations just as in the even-parity data. Again, the measured resonance positions are defined by easily identified characteristics. In this case, we measured the positions of the peaks of the resonance profiles. Estimated random errors for these measurements are typically $\sim \pm 0.5$ cm^{-1}.

III. SEMICLASSICAL THEORY

The interpretation of the spectrum in the strong-mixing regime is only partly developed, and in this paper we concentrate on its coarsest feature, the quasi-Landau resonances. The basic theoretical problem is that the Schrödinger equation for the valence electron of a hydrogen-like atom in a strong magnetic field is nonseparable. When the combined magnetic and Coulomb fields are of comparable strength, perturbation theory is not applicable and other approximations must be employed. A simplification comes from noting that the system is cylindrically symmetric, and hence parity and the magnetic quantum number M remain good quantum numbers for all values of B. Following Starace,[10] we write the electron's wave function in cylindrical coordinates as

$$\Psi(\rho,\phi,z) = \rho^{-1/2} f(\rho,z) e^{iM\phi} \quad \text{for } M = 0, \pm 1, \pm 2, \ldots . \tag{1}$$

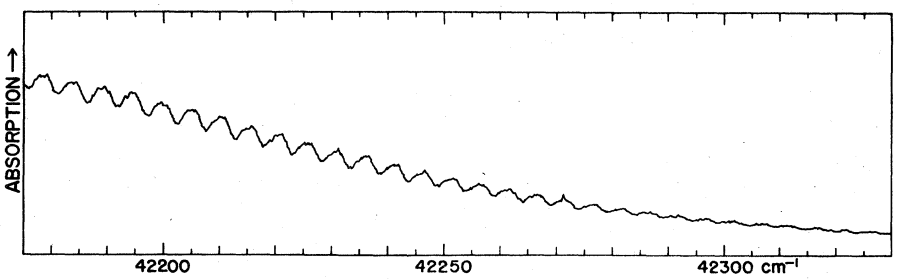

FIG. 3. Portion of densitometer trace of odd-parity absorption spectrum of Ba I showing resonances extending to 250 cm^{-1} above the limit. $B=46.7$ kG, $M=-1$.

The spin-independent Schrödinger equation for hydrogen with a uniform magnetic field in the z direction is

$$\frac{\partial^2 f}{\partial \rho^2}+\frac{\partial^2 f}{\partial z^2}+\frac{2m}{\hbar^2}[\epsilon - V(\rho,z)]f=0\,, \tag{2}$$

where

$$V(\rho,z)=\frac{\hbar^2}{2m}\frac{(M^2-1/4)}{\rho^2}-\frac{e^2}{4\pi\epsilon_0(\rho^2+z^2)^{1/2}}+\tfrac{1}{2}m\alpha^2\rho^2$$

and

$$\epsilon = E-\alpha\hbar M\,.$$

In the above, E is the electron energy referred to the $B=0$ ionization limit, $\alpha\hbar M$ is the energy due to the orbital magnetic moment of the electron in the magnetic field, and $\alpha=eB/2m$ is half the cyclotron frequency $\omega_c=eB/m$. The effective potential $V(\rho,z)$ contains centrifugal, Coulomb, and diamagnetic Zeeman terms.

It is apparent from the appearance of the spectra in Figs. 2 and 3 that the electron motion is strongly influenced by the harmonic diamagnetic potential term in the region around $E\approx 0$. In this region, the cyclotron frequency ω_c characterizes the electron motion in directions perpendicular to the magnetic field, and it is much greater than the frequency of the motion of the electron in the Coulomb potential along the magnetic field lines. Noting this, Schiff and Snyder[17] suggested the adiabatic approximation as a means of decoupling the electron motion in the ρ and z directions, and several authors have applied this approximation to very high magnetic field studies.[1] In this approximation, the electron behavior along the field axis (i.e., in the z direction) is governed by the Coulomb potential averaged over the (ρ,ϕ) plane for each value of z. The extreme application of this approach is to ignore the dependence on the z direction altogether. In addition, Fano[18] has noted that the cresting of the effective potential $V(\rho,z)$ in the $z=0$ plane causes the probability density distribution for certain states to concentrate in that plane, suggesting that a useful lowest-order approximation is to consider motion in the $z=0$ plane only.

Accordingly, we set $z=0$, and the radial part of the two-dimensional Schrödinger equation in polar coordinates (ρ,ϕ) is obtained from Eq. (2):

$$\frac{d^2F(\rho)}{d\rho^2}+\left(2\epsilon-\frac{M^2-1/4}{\rho^2}+\frac{2}{\rho}-\alpha^2\rho^2\right)F(\rho)=0\,, \tag{3}$$

where we have switched to atomic units ($m=e=\hbar=1$) for convenience. For highly excited states, the WKB approximation provides the eigenvalues ϵ of Eq. (3). Akimoto and Hasegawa[19] have considered the applicability of this approximation to Eq. (3) and concluded that, for all values of M, the quantum condition for bound eigenstates is

$$\int_{\rho_1}^{\rho_2}\left(2\epsilon-\frac{M^2}{\rho^2}+\frac{2}{\rho}-\alpha^2\rho^2\right)^{1/2}d\rho$$
$$=(\tilde{n}+\tfrac{1}{2})\pi \quad \text{for } \tilde{n}=0,1,2,3,\ldots\,. \tag{4}$$

Here ρ_1 and ρ_2 are the turning points of the classical motion and are given by the zeros of the integrand.

The centrifugal potential has been modified by the addition of a term $-\frac{1}{4}\rho^2$ in order that the WKB approximation be valid for all $\rho\geq 0$. In general, Eq. (4) is numerically integrated to obtain the energy E as a function of the radial quantum number $\tilde{n}$.

In the absence of the ionic core (high-field limit), it is easily verified that the energy levels given by Eq. 4 are precisely the spinless Landau levels for $p_z=0$,

$$E=[\tilde{n}+(M+|M|+1)/2]\hbar\omega_c\,, \tag{5}$$

where $\tilde{n}$ plays the role of the Landau radial quantum number N^1. For $B=0$ on the other hand, Eq. (4) yields a quasihydrogenic spectrum given by

$$E=-[2(\tilde{n}+|M|+\tfrac{1}{2})^2]^{-1}\,.$$

The half-integral radial quantum number is a result of applying a two-dimensional model appropriate to the Landau regime to the three-dimensional Coulomb problem.

Economou, Freeman, and Liao[5] sought to obtain the correct Coulomb limit by replacing the two-dimensional centrifugal potential in Eq. (4) by $(M+\frac{1}{2})^2/\rho^2$, which is of the usual three-dimensional type. This substitution, however, results in integer Landau quantum numbers. It does not appear to be possible to obtain both limits correctly with a simple WKB formalism. Interestingly, for the spin-$\frac{1}{2}$ atom (Rb I) studied by Economou *et al.*, the orientation energy of the spin magnetic moment in the magnetic field is $\pm\frac{1}{2}\hbar\omega_c$, so that the Landau levels including spin are in fact integer multiples of $\hbar\omega_c$. In the present case ($S=0$), no such accidental compensation occurs and it seems preferable to retain the two-dimensional centrifugal potential.

This two-dimensional WKB model describes the bound states as evolving continuously from the Coulomb energy levels at low $\tilde{n}$ through the quasi-Landau region ($E\approx 0$) to the Landau levels at very high energies. The QLRs are depicted as highly excited bound states characterized by a single radial quantum number $\tilde{n}$. These states appear to evolve smoothly out of the Coulomb-Rydberg levels with increasing energy, and successively lower $\tilde{n}$ values are raised across the $B=0$ ionization

threshold as B is increased. The actual situation is much more complicated, with each resonance below the limit comprising many individual diamagnetically mixed bound levels, but it is shown below that this model successfully describes the spacing and B dependence of the quasi-Landau resonance energies.

For $M=0$, the quantization rule reduces to

$$\int_0^{\rho_2} (2E+2/\rho-\alpha^2\rho^2)^{1/2}\,d\rho=(\tilde{n}+\tfrac{1}{2})\pi\,, \tag{6}$$

where ρ_2 is the real root of the integrand. At the zero-field ionization limit, $E=0$ and $\rho_2=(a/\alpha^2)^{1/3}$. Equation (6) is the basic equation with which we compare our measurements of the quasi-Landau resonances.

The WKB energy levels in the region where the Coulomb field is dominant (but with $B\neq 0$) are easily obtained for $M=0$. For small values of B, we expand

$$E\approx E(\alpha^2=0)+\alpha^2\frac{\partial E}{\partial\alpha^2}\Big|_{\alpha^2=0}\,,$$

where $\partial E/\partial\alpha^2$ is obtained from the derivative of Eq. (6). The result is

$$E=-1/2(\tilde{n}+\tfrac{1}{2})^2+\tfrac{5}{4}(\tilde{n}+\tfrac{1}{2})^4\alpha^2\,, \tag{7}$$

in agreement with Akimoto and Hasegawa.[19] These are just Rydberg levels with a first-order diamagnetic Zeeman shift. The first-order correction in the energy has the usual n^4B^2 scaling of the diamagnetic Zeeman shift, although the magnitude of the correction differs by factors of ~2 from the values obtained using first-order perturbation theory with hydrogenic wave functions.[1]

A modified Bohr atomic model of the strong-mixing regime has been discussed by Canuto and Kelly[20] and by Garstang.[1] It is interesting to compare this model to the WKB calculations and to our experimental results. Consider a Bohr atom in a uniform magnetic field with an electron in a circular orbit of radius r around an infinitely massive ion core (net charge $=+e$) with the orbital plane perpendicular to the magnetic field. The force, angular momentum, and energy relations govern the electronic motion and result in the following coupled equations for the energy as a function of principal quantum number n:

$$n^2=(r/R)^4+r/a_0\,, \tag{8}$$

$$E=\alpha(n+r^2/R^2-R^2/2a_0r)\,, \tag{9}$$

where $\alpha=\hbar\omega_c/2$, a_0 is the Bohr radius, and $R=(\hbar/\alpha m)^{1/2}$ is the quantum electron gyroradius. In practice, E as a function of n is obtained by numerically solving Eqs. (8) and (9).

In the absence of a magnetic field, Eqs. (8) and (9) reduce to the usual hydrogenic levels ($E=-\mathcal{R}_\infty/n^2$), where $\mathcal{R}_\infty$ is the Rydberg constant), while if the ion core is absent, the energy levels are Landau-like levels with the energy given by $E=n\hbar\omega_c=2n\alpha$. Thus this simple Bohr model results in a set of energy levels which have approximately the proper behavior at both very small and very large magnetic field strengths. In addition, it describes a smooth transition from the Coulomb regime through the strong-mixing regime to the Landau regime with the energy levels again being described with a single quantum number n, which is similar to the picture provided by the WKB model.

An even simpler semiclassical calculation has been advanced by O'Connell[21] to describe the coarse structure of the spectrum in the region $E\gtrsim 0$. Again, one considers an electron in a circular orbit around the ion core in a plane perpendicular to the magnetic field. The energy is written as a sum of contributions from the magnetic and Coulomb fields. For high excitation, the magnetic field dominates and the effect of the Coulomb field on the orbital radius is taken to be negligible. The magnetic contribution to the total energy is just the Landau energy, while the Coulomb interaction energy between the electron and ionic core is evaluated for an orbital radius equal to that of a free electron in a homogeneous magnetic field. The total electron energy is then given by

$$E=2\alpha[n-K(B_0/2nB)^{1/2}]\,, \tag{10}$$

where

$$B_0\equiv\hbar/ea_0^2=2.3505\times10^6\,\mathrm{kG}\,.$$

Equation (10) is just the Landau energy level with a first-order perturbation due to the presence of the ionic core. This result does not have the proper behavior in the Coulomb limit. We have included an additional numerical constant factor K in the second term of Eq. (10) with the anticipation that Eq. (10) has approximately the correct n dependence near $E=0$ but that these semiclassical expressions are uncertain by unknown numerical factors of order unity.[3] Below, we adjust K to provide a best fit to our data.

Simple models like these are useful in determining the scaling of parameters such as dE/dn and $n(E=0)$ with magnetic field strength, and for estimating the values of n at which the strong-mixing regime occurs for a given value of B. However, absolute numerical values obtained from expressions such as Eqs. (8) and (9) and from Eq. (10) are not to be taken very seriously.

For the purpose of comparing all of the above semiclassical expressions for the quasi-Landau resonance energies with each other and with experimental results, we have found it convenient to rewrite the equations in such a way that explicit dependence on the magnetic field strength is eliminated. To that end, we define the new variables

$$E' = E\alpha^{-2/3}, \tag{11a}$$

$$n' = \begin{cases} (\tilde{n}+\frac{1}{2})\alpha^{1/3} & \text{(WKB and Landau)} \\ n\alpha^{1/3} & \text{(all other models)}, \end{cases} \tag{11b}$$

$$s = r\alpha^{2/3}. \tag{11c}$$

Using these new variables and working in atomic units, Eqs. (6), (8), (9), and (10) become, respectively,

$$\int_0^S (2E' + 2/s - s^2)^{1/2}\, ds = n'\pi \quad \text{(WKB: } M=0), \tag{12}$$

$$(n')^2 = s^4 + s, \tag{13a}$$

$$E' = n' + s^2 - \tfrac{1}{2}s^{-1}, \quad \text{(Bohr)} \tag{13b}$$

$$E' = 2n' - K(n')^{-1/2} \quad \text{(O'Connell)}, \tag{14}$$

We include the Coulomb and Landau [Eq. (5)] cases for completeness:

$$E' = -1/2n'^2 \quad \text{(Coulomb)}, \tag{15}$$

$$E' = 2n' \quad \text{(Landau)}. \tag{16}$$

In Eq. (12), S is the real root of the integrand. With this transformation, the numerical calculations need be performed only once, and the results for arbitrary values of the magnetic field B are obtained via Eqs. (11). In addition, we will see below that using Eqs. (11) to scale our measurements of the energies of the QLRs allows us to condense data obtained over a range of B values to a single unified plot.

So far, all energies have been referred to the zero-field ionization limit. It is necessary to specify "zero-field" because, in general, the ionization potential is a function of B. In the case of the alkaline earths, and for experimentally realizable fields, the ground states of the atom ($^1S_0$) and of its residual ion ($^2S_{1/2}$) have negligible diamagnetic shifts. Since in both cases the orbital angular momentum $L=0$, any linear Zeeman shifts must be due entirely to spin. Assuming spin conservation in the ionization process, the only magnetic contribution to the ionization potential is that of the final-state continuum electron, i.e., its Landau energy (not including spin).

The lowest value of this energy, using Eq. (5), then gives the increase in ionization potential caused by the external magnetic field:

$$\Delta E_I = \begin{cases} \frac{1}{2}\hbar\omega_c, & M \le 0 \quad \text{(17a)} \\ (M+\frac{1}{2})\hbar\omega_c, & M > 0. \quad \text{(17b)} \end{cases}$$

In the present cases ($M=0$ and -1), the threshold is thus expected to be shifted upward slightly, by $\frac{1}{3}$ of a QLR spacing. This is too small a shift to be readily observable spectroscopically.

IV. RESULTS

In this section we compare our measurements of the QLR energies to the results of the semiclassical theories discussed above. We consider the WKB model first. Also, we concentrate on the region near and above the $B=0$ ionization limit since the spectra at lower energies are Rydberg levels with the diamagnetic Zeeman effect as a perturbation and, in principle at least, are well understood.[1,4,6,22] For the present analysis, the value of $\tilde{n}$ must be determined for at least one resonance at one field strength for each case (i.e., each atomic species at a given parity and value of M). To that end, we simply assign a value of $\tilde{n}$ to one resonance at one field strength such that the interpolated value of $\tilde{n}$ at $E=0$ agrees with that calculated from Eq. (5). The value of $\tilde{n}$ assigned in this manner is not required to be an integer because the measured position of a given resonance is dependent on its profile and the WKB model ignores such effects as the presence of a nonhydrogenic ion core and the coupling of motion to the z direction, which gives rise to the complex shapes of the resonances. We only require that the values of $\tilde{n}$ for adjacent resonances differ by unity. With this definition for a single datum point, the $\tilde{n}$ values of all the resonances are fixed for all values of B, since the motion of individual resonances can be traced over the full range of magnetic field strengths studied. The question is now whether all other data points agree with Eq. (5).

For example, consider the case of Sr I ($M=0$, even parity) at $B=40$ kG [Fig. 2(b)]. The ionization limit was found to lie above the lower of the two peaks which straddle the limit by 0.60 ± 0.05 times the total energy spacing between the two peaks. The corresponding result for the resonance minimum in Ba I at $B=40$ kG is 0.55 ± 0.05. Since Eq. (6) gives $\tilde{n}$ ($E=0$) $=44.58$ at $B=40$ kG, we assign $\tilde{n}=44.0$ to both the first resonance peak below the limit for Sr I and the first minimum be-

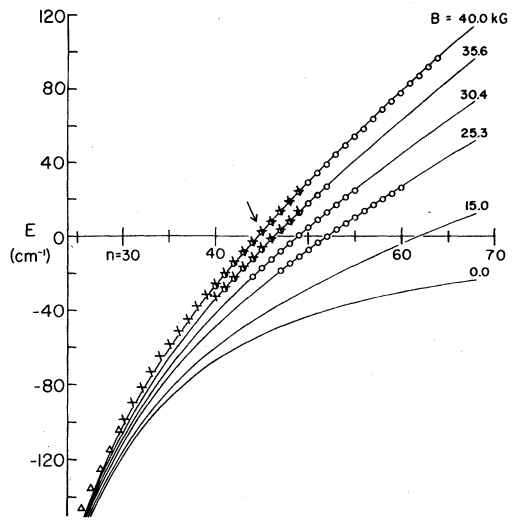

FIG. 4. Resonance positions as a function of $\tilde{n}$ for the $M=0$ even-parity ionization spectra. ○ Sr I resonance-peak positions; × Ba I resonance-minimum positions; △ Ba I peak positions. The lowest datum point corresponds to the diamagnetically mixed $6s31s\ ^1S_0$ line complex.

low the limit for Ba I. Because the fine structure becomes quite complex at energies well below $E=0$ in the Ba I spectrum at $B=40$ kG, it was more convenient to define the resonance positions in this region by the peaks of the profiles, with the peaks accordingly assigned half-integral $\tilde{n}$ values.

A plot of the measured energies of the resonances as a function of $\tilde{n}$ for a few values of B is shown in Fig. 4 for the $M=0$ ionization spectra (Fig. 4 is a reproduction of Fig. 3 in Ref. 7). The solid lines are obtained from numerical integration of Eq. (6). The measured values of B have a total uncertainty of $\sim\pm0.2$ kG. The one datum point for each element whose $\tilde{n}$ value is defined to agree with Eq. (5) is indicated by the arrow.

The general agreement between measurements and the WKB calculations is evident. At the lowest energies observed in Ba I, the QLR merge into the diamagnetically shifted and mixed Rydberg spectrum, where the $6s\ 31s\ ^1S_0$ line complex is identified (no even-parity observations for Sr I were made in this energy region). Even though the electronic motion is no longer dominated by the magnetic field at these lower energies, qualitative agreement with the two-dimensional WKB model is not surprising because, as noted earlier, the WKB results yield the usual hydrogenic energy levels plus a diamagnetic shift term with the proper $n_c^4B^2$ dependence. Our assignment of the $\tilde{n}$ value at the ionization limit is checked for consistency with the semiclassical picture of the QLR evolving from the Rydberg levels at lower energies by noting that the Ba I $6s\ 31s\ ^1S_0$ level has been assigned $n_c=\tilde{n}+\frac{1}{2}=26.0$ by extrapolation from the limit, while its effective quantum number at $B=0$ is $n^*=n-\mu=26.8$ (the quantum defect $\mu=4.2$ for the $6sns\ ^1S_0$ series of Ba I). The agreement between n^* and n_c is satisfactory when one notes that the simple two-dimensional WKB model ignores such effects as electron-ion core interactions, the presence of a second valence electron in Ba I which gives rise to a relatively complex spectrum in the region where the Coulomb field dominates,[6,23] and coupling of electron motions parallel and perpendicular to the magnetic field lines, which is manifested in part by the complex resonance profiles and fine structure. The diamagnetic interaction between the $6sns\ ^1S_0$ and $6snd\ ^1D_2$ Rydberg series as the spectrum evolves into the quasi-Landau regime[6] allows for an ambiguity of ~1 in the assignment of $\tilde{n}$ as the energy increases. Recently, Economou, Freeman, and Liao[5] have reduced the ambiguity in the connection between the zero-field radial quantum number and $\tilde{n}$ to about 0.3 by studying the evolution of Rydberg levels into the quasi-Landau structure at $E<0$ in the simpler case of Rb I.

Historically, much interest in the quasi-Landau resonances has centered upon $E=0$. In their paper, Garton and Tomkins[8] reported that the spacing between resonances at $E=0$ was $\sim1.5\ \hbar\omega_c$ for $B=24$ kG. Using the derivative of Eq. (4), Starace showed, by numerical integration, that $dE/d\tilde{n}=1.50\ \hbar\omega_c$ for $M=\pm1$ and $\epsilon=0$, and he found that this result was independent of B. After a straightforward calculation, the derivative of the $M=0$ WKB integral in Eq. (6) yields analytically[13]

$$\frac{dE}{d\tilde{n}}=\tfrac{3}{2}\hbar\omega_c \quad \text{for } E=0\,, \tag{18}$$

which agrees with the calculated results for $M=1$. Equation (18) also is obtained from O'Connell's result (10) for arbitrary value of the constant K. The energy difference between the two resonances straddling the ionization limit is plotted in Fig. 5 for the ionization-spectra results. The data agree within their uncertainty with Eq. (18), which is plotted as the solid line in the figure

$$(3\hbar\omega_c/2B=0.1401\ \text{cm}^{-1}/\text{kG})\,.$$

The error bars in Fig. 5 were assigned assuming a random uncertainty of ±0.2 cm^{-1} for each measurement. The total uncertainty in each value of B is typically ±0.2 kG, although relative values of B are good to ±0.1 kG.

Using a semiclassical approach similar to that of O'Connell, Rau[2] predicted a $B^{-1/3}$ scaling for

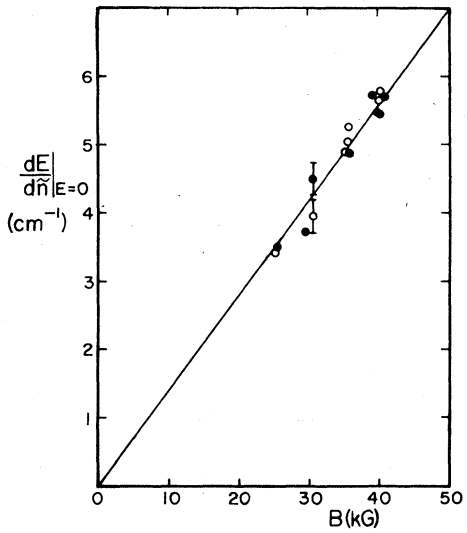

FIG. 5. Resonance spacing at the ionization limit as a function of magnetic field strength. ● Sr I, ○ Ba I. Both even parity, $M=0$. Solid line is $dE/d\tilde{n}=1.5\,\hbar\omega_c$.

n at $E=0$. Setting $E=0$ and $s=\alpha^{2/3}\rho$, Eq. (6) becomes

$$\tilde{n}\,(E=0)+\tfrac{1}{2}=\alpha^{-1/3}\frac{1}{\pi}\int_0^{2^{1/3}}\left(\frac{2}{s}-s^2\right)^{1/2}ds\,, \qquad (19)$$

where the integral equals 2.891. For $\tilde{n}\gg\frac{1}{2}$, this gives $n(E=0)$ proportional to $B^{-1/3}$, in agreement with Rau's result. The value of $\tilde{n}(E=0)$ is plotted as a function of B in Fig. 6 for the Sr I data. The solid line is given by Eq. (21), and the one datum point defined to agree with theory is again noted by the arrow. A linear least-squares fit of $\ln[\tilde{n}(E=0)+\frac{1}{2}]$ vs $\ln B$ for these data gives a slope of -0.334 ± 0.001 and an intercept of 5.041 ± 0.003, while Eq. (19) predicts $-\frac{1}{3}$ and 5.038, respectively. Similar results are obtained for the Ba I data. We note here that results given in Figs. 5 and 6 are contained implicitly in Fig. 4, but the

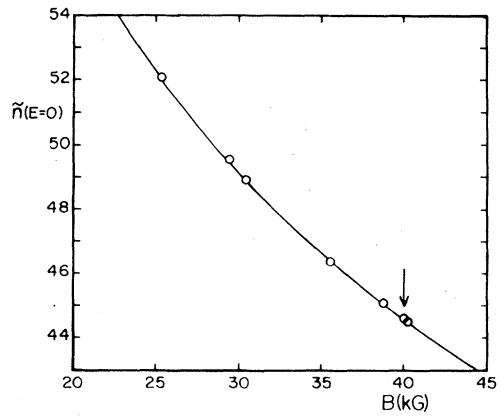

FIG. 6. $\tilde{n}(E=0)$ vs B for Sr I even parity, $M=0$.

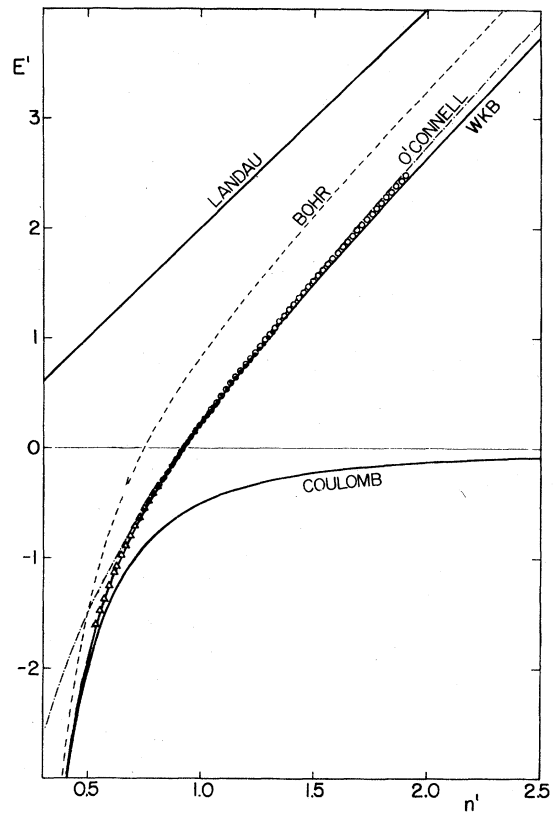

FIG. 7. Normalized resonance positions E' vs normalized radial quantum number n'. ● Sr I even parity $M=0$, $B=25$–40 kG; △ Ba I even parity $M=0$, $B=40$ kG; ○ Ba I odd parity $M=-1$, $B=46.7$ kG. Normalized versions of various models [Eqs. (12)–(16)] are also shown.

former plots show this agreement with the WKB results in more detail than the latter.

The agreement between measurement and theory in Fig. 6 verifies that the scaling used in Eq. (11) is indeed correct. It also suggests a criterion for selecting a value of the numerical constant K in Eq. (10): We require that $n(E=0)=45.08$ at $B=40$ kG in accordance with the WKB calculations so that the agreement between the data and the model for $n(E=0)$ vs B is as good as that shown in Fig. 6. The value of K thus obtained is $K=1.766$.

Using Eq. (11) to scale the measured values of $\tilde{n}$ and E for all available data, our results collapse to the single plot shown in Fig. 7. For convenience, we have included the Ba I ($M=-1$) absorption data here by treating it as if $M=0$ for the purpose of assigning $\tilde{n}(E=0)$ and calculating E vs $\tilde{n}$. This is valid because it was found that changing M by one in Eq. (4) resulted in numerically changing $\tilde{n}$ by one to an accuracy of a few percent. This allows our comparison between data and theory to be extended appreciably in energy above $E'=0$. The results in Fig. 7 indicate that

the WKB model works quite well over the full range of energies observed. For $E' \gtrsim 0$, the O'Connell model is also surprisingly accurate considering its simplicity. The deviation between it and the data at low E' is indicative of its failure to converge to the proper Coulomb energies $\sim n'^{-2}$ at low n'. The modified Bohr model is not as accurate in the region around $E=0$ but has the virtue of achieving the proper limiting behavior of dE/dn at both high and low E'. It is also useful for crude estimates of orbital radii in the strong-mixing regime. The slight deviation of the Ba I odd-parity absorption data from the WKB curve is not considered significant since we have ignored possible systematic errors arising from collisional effects, motional Stark effects, or changes in the resonance profiles at increasing energies. In addition, the influence of the $5d8p\,{}^1P_1{}^0$ doubly excited level, which bridges the first ionization limit, has not been considered.

V. DISCUSSION

The agreement between the measurements and the two-dimensional hydrogenic WKB model is quite good over the full range of energy and B values observed. The predictions of a $1.5\,\hbar\omega_c$ spacing at $E=0$ and a $B^{-1/3}$ scaling of $[\tilde{n}(E=0)+\frac{1}{2}]$ are both verified by our measurements. Considering the complexity of the $B=0$ spectra of Ba I and Sr I, the experimental results are consistent with the depiction of the WKB radial quantum number $\tilde{n}$ evolving smoothly from the Coulomb radial quantum number at low energies. The simple formula derived by O'Connell works quite well in describing the energies of the resonances for $E \gtrsim 0$, partly because we have adjusted it to agree with the WKB results at the limit. It does provide a convenient estimate of E and dE/dn for the region $E \gtrsim 0$. However, since it breaks down for $E<0$, the connection between the lower bound states and the the quasi-Landau resonances does not occur in this model.

Since the resonance positions are determined by the behavior of the effective potential $V(\rho, z=0)$ over a large range of ρ, they are little affected by the electron-ion interaction at small ρ, and hence are independent of atomic species, aside from a quantum defect shift. However, the resonance profiles are strongly species dependent, as seen in Fig. 2 and other studies.[5,15,16] The spherically symmetric Coulomb potential couples the motion of the electron in the ρ direction to that in the z direction. If the total energy is above the ionization limit, the electron can escape by autoionizing into an orbit along the z axis.[10] The Coulomb potential due to the ion core is largest near the origin, and hence the coupling between the motion in the ρ and z directions is sensitive to the electron wave function near the ion core. Thus the resonance profiles will be dependent on the atomic species studied. The detailed analysis of the resonance profiles and fine structure is complex and beyond the scope of this work.

We have observed the quasi-Landau resonances in $M=0$ even-parity and $M=\pm1$ odd-parity spectra, and they also appear in $M=\pm2$ even-parity[5] spectra. Since the resonance structure is quite dependent on the wave function of the $z=0$ plane, they should be most prominent in states whose wave functions have an antinode at $\theta=\pi/2$ in spherical coordinates (i.e., the $z=0$ plane), and much less so for states with a node in that plane.[18] If Π denotes the usual parity of a given state, the magnetic parity for reflection through the $\theta=\pi/2$ plane is given by $\Pi+|M|$. For $M=0$ and odd parity, $\Pi+|M|$ is odd and a node occurs at $\theta=\pi/2$, indicating that the resonance structure should not occur. Likewise, antinodes are present at $\theta=\pi/2$ for $M=\pm1$ odd-parity and $M=0$, ±2 even-parity states, indicating that the resonances should occur since $\Pi+|M|$ is even. The absence of clearly observed resonances in σ-polarization spectra in our experiment is most likely due to the superposition of the $M=0$, $+2$, and -2 spectra in the transverse field. Further observation to test for the appearance or lack of appearance of quasi-Landau resonances in the $M=\pm1$ even-parity spectra would be useful in further testing this even-magnetic-parity selection rule.

As emphasized by Rau,[24] the magnetic case studied here is but one example of the more general problem of strong-field-mixing effects that arise in many physical situations. The observation of equally spaced resonances near the zero-field ionization limit in the presence of an external electric field[25] is another such example, and similar phenomena are expected in systems of two-dimensional electron layers at the surface of liquid helium in the presence of electric and magnetic fields. In all of these cases, semiclassical models similar to those used here are applicable.

Of course, these simple models are inadequate for understanding the details of the diamagnetic structure observed here and in other experiments,[8,16,22] and theoretical developments directed toward quantitatively explaining the resonance profiles and superposed fine structure are needed. Further experiments at higher magnetic fields would be useful in elucidating the correlation of the fine structure to the zero-field levels, but such efforts will have to be more sophisticated than the present survey work in order to avoid complicating factors such as the motional Stark effect and the presence of a nonhydrogenic ion core.

ACKNOWLEDGMENTS

D. C. Wright aided in much of the experimental work, and B. Ercoli provided technical assistance. W. R. S. Garton of Imperial College, London, provided the superconducting magnet, which was constructed at Rutherford Laboratory. One of the authors (RJF) acknowledges support of the NSF. This work was supported in part by the Division of Basic Energy Sciences of the U.S. Department of Energy.

---

*Present address: Plasma Physics Laboratory, Princeton Univ., Princeton, N.J. 08540.

[1]R. H. Garstang, Rep. Prog. Phys. 40, 105 (1977).
[2]A. R. P. Rau, Phys. Rev. A 16, 613 (1977).
[3]R. F. O'Connell, Phys. Rev. A 17, 1984 (1978).
[4]M. L. Zimmerman, J. C. Castro, and D. Kleppner, Phys. Rev. Lett. 40, 1083 (1978).
[5]N. P. Economou, R. R. Freeman, and P. F. Liao, Phys. Rev. A 18, 2506 (1978).
[6]R. J. Fonck, F. L. Roesler, D. H. Tracy, K. T. Lu, F. S. Tomkins, and W. R. S. Garton, Phys. Rev. Lett. 39, 1513 (1977).
[7]R. J. Fonck, D. H. Tracy, D. C. Wright, and F. S. Tomkins, Phys. Rev. Lett. 40, 1366 (1978).
[8]W. R. S. Garton and F. S. Tomkins, Astrophys. J. 158, 839 (1969).
[9]A. R. Edmonds, J. Phys. Paris 31 (C4), 71 (1970).
[10]A. F. Starace, J. Phys. B 6, 585 (1973).
[11]D. Popescu, M. L. Pascu, C. B. Collins, B. W. Johnson, and I. Popescu, Phys. Rev. A 8, 1666 (1973); J. A. Armstrong, P. Esherick, and J. J. Wynne, *ibid.* 15, 180 (1977).
[12]P. Esherick and J. J. Wynne, Comments At. Mol. Phys. 7, 43 (1977).
[13]R. J. Fonck, Ph.D. thesis, University of Wisconsin, 1978 (unpublished).
[14]M. Rosenbluh, T. A. Miller, D. M. Larsen, and B. Lax, Phys. Rev. Lett. 39, 874 (1977).
[15]H. Crosswhite, U. Fano, K. T. Lu, and A. R. P. Rau, Phys. Rev. Lett. 42, 963 (1979).
[16]K. T. Lu, F. S. Tomkins, and W. R. S. Garton, Proc. R. Soc. London A 362, 421 (1978).
[17]L. I. Schiff and H. Snyder, Phys. Rev. 55, 59 (1939).
[18]U. Fano, Colloq. Int. C.N.R.S. 273, 127 (1977).
[19]O. Akimoto and H. Hasegawa, J. Phys. Soc. Japan 22, 181 (1967).
[20]V. Canuto and D. C. Kelly, Astrophys. and Space Sci. 17, 277 (1972).
[21]R. F. O'Connell, Astrophys. J. 187, 275 (1974).
[22]K. T. Lu, F. S. Tomkins, H. M. Crosswhite, and H. Crosswhite, Phys. Rev. Lett. 41, 1034 (1978).
[23]J. R. Rubbmark, S. A. Borgstrom, and K. Bockasten, J. Phys. B 10, 421 (1977).
[24]A. R. P. Rau, J. Phys. B 12, L193 (1979).
[25]R. R. Freemen, N. P. Economou, G. C. Bjorklund, and K. T. Lu, Phys. Rev. Lett. 41, 1463 (1978).